NASA CONTRACTOR REPORT

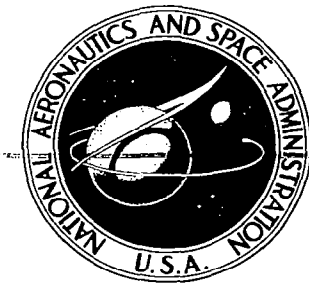

NASA CR-900

FORE-AND-AFT STIFFNESS CHARACTERISTICS OF PNEUMATIC TIRES

by R. N. Dodge, David Orne, and S. K. Clark

Prepared by
THE UNIVERSITY OF MICHIGAN
Ann Arbor, Mich.
for

NATIONAL AERONAUTICS AND SPACE ADMINISTRATION • WASHINGTON, D. C. • OCTOBER 1967

NASA CR-900

FORE-AND-AFT STIFFNESS CHARACTERISTICS OF PHEUMATIC TIRES

By R. N. Dodge, David Orne, and S. K. Clark

Issued by Originator as Technical Report No. 6

Prepared under Grant No. NsG-344 by
THE UNIVERSITY OF MICHIGAN
Ann Arbor, Mich.

for

NATIONAL AERONAUTICS AND SPACE ADMINISTRATION

For sale by the Clearinghouse for Federal Scientific and Technical Information
Springfield, Virginia 22151 – CFSTI price $3.00

TABLE OF CONTENTS

LIST OF ILLUSTRATIONS

LIST OF ILLUSTRATIONS (Continued)

I. INTRODUCTION

Pneumatic tires are functional parts of many dynamic systems. In order to effectively design and engineer such systems, it is often necessary to know the mechanical properties of the component parts, including the tires. One of the major roles of this research group has been to study and analyze some of the important mechanical properties of pneumatic tires and to present rational methods for predicting them.

Several paths have been followed by this research group in developing approximate methods for predicting mechanical properties of tires. One technique involved modeling of the penumatic tire as a cylindrical shell supported by an elastic foundation.[5-7] This model gives relations for predicting several properties involving deformation in the plane of the wheel, such as contact patch length vs. vertical deflection, vertical load vs. vertical deflection, plane vibration characteristics, transmissability characteristics, and dynamic response to a point load.

A more recent attempt[4] involved analyzing the pneumatic tire as a string on an elastic foundation. This model is primarily used to predict lateral stiffness characteristics, vertical stiffness characteristics and twisting moments. However, it has been found to be useful only when the inflation pressure is high, such as in the case of aircraft tires.

This report presents a method for predicting the fore-and-aft stiffness characteristics of pneumatic tires. Fore-and-aft properties are important in the overall analysis of a tire since they represent the contributions of

the carcass and tread to braking and tractive elasticity. A different model is required here since neither the cylindrical shell nor the string on the elastic foundation provide means for transmitting such loads. It is hoped that this model will prove satisfactory for predicting fore-and-aft characteristics of various tire designs.

II. SUMMARY

An elastic bar supported by a foundation exhibiting elasticity in shear serves as a model for determining the fore-and-aft stiffness properties of a pneumatic tire. The differential equation representing the deformation is derived and solved, and the resulting solution gives a means for calculating a fore-and-aft spring rate for the model.

A series of five tires of various sizes and structures was used for testing the validity of the proposed model. A set of static tests was performed to establish an experimental value for the fore-and-aft spring-rate for the various tires. Additional structural data, required by the analytical solution of the model, were also obtained from the tires. A comparison of the calculated and experimental results was reasonably satisfactory, indicating that the proposed model can be used to roughly approximate fore-and-aft stiffness characteristics.

A complete tabular summary of the geometry and composition of the five tires is included for easy reference. All experimental and analytical results are summarized and compared in graphical form.

III. ANALYSIS

To represent fore-and-aft stiffness characteristics, the pneumatic tire is idealized as an elastic bar supported by an elastic shear foundation (see Figure 1). The elastic bar portion of the model represents the tread region of the tire which is loaded by the fore-and-aft load F. In addition to the restraint offered by the stiffness of the tread region itself, resistance to deformation by the load F is provided by the tires' ability to withstand shearing forces in the sidewall regions. This portion of the tire is represented in the model by the elastic shear foundation.

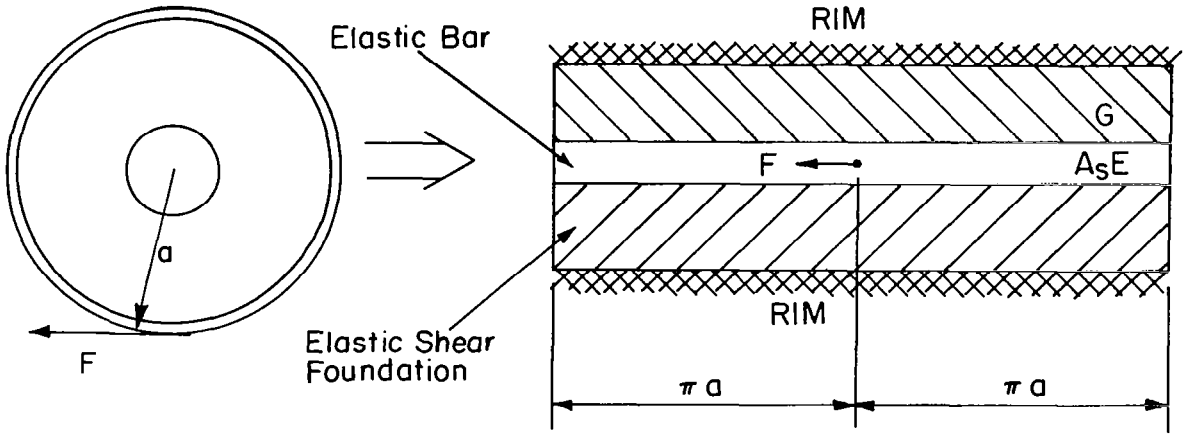

Figure 1. Idealized model of pneumatic tire for analyzing fore-and-aft spring rates.

If it is assumed that the restraining force of the elastic shear foundation is directly proportional to the displacement, an elemental segment of the elastic bar can be set in equilibrium as shown in Figure 2. Note that ad-

vantage is taken of the symmetry present in the model.

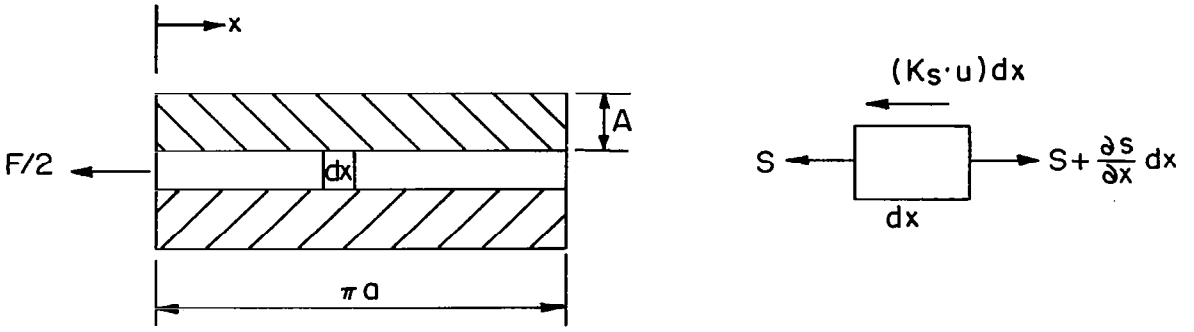

Figure 2. Loaded element of a portion of the model.

In Figure 2, S is the force acting on the bar, u is the displacement, and K_S is the spring rate per unit length of the shear foundation. It is assumed that K_S is provided only by the shear resistance of the sidewall. From Figure 2, it is seen that one may approximate

$$K_S = \frac{2GH}{A}$$

where G is the effective shear modulus of the sidewall, H is the sidewall thickness, and A is the length along the sidewall from the rim to the point of intersection of the tread and carcass.

From equilibrium of the element,

$$\frac{\partial S}{\partial x} - K_S u = 0$$

$$S = TA_S = EeA_S = A_S E \frac{\partial u}{\partial x}$$

where T is the stress, e the resulting strain, A_s the cross-sectional area of the bar at any location, and E the effective extension modulus of the tread region in the circumferential direction. Thus,

$$\frac{\partial^2 u}{\partial x^2} - q^2 u = 0 \qquad (1)$$

where

$$q^2 = \frac{K_s}{A_s E}$$

The general solution of this equation is

$$u = C_1 \cosh qx + C_2 \sinh qx \qquad (2)$$

The boundary conditions for this problem are determined by assuming that each half of the tire (fore-and-aft of the contact patch) is equally loaded, so that

$$\text{at} \quad x = 0, \quad S = \frac{F}{2}$$

$$\text{at} \quad x = \pi a, \quad S = 0 \qquad (3)$$

Substituting (3) into (2) gives

$$C_1 = \frac{-F}{2A_s E \tanh \pi aq}; \qquad C_2 = \frac{F}{2A_s Eq} \qquad (4)$$

Thus,

$$u(x) = \frac{F}{2A_s Eq}\left[\sinh qx - \frac{\cosh qx}{\tanh q\pi a}\right] \qquad (5)$$

The fore-and-aft stiffness is determined by finding the ratio of the applied load to the displacement at the point of application of the load. Thus,

$$K_f = \left| \frac{F}{u(o)} \right| = \left| - 2A_s Eq \, (\tanh q\pi a) \right| \qquad (6)$$

Equation (6) now represents a relationship for the fore-and-aft spring-rate of a pneumatic tire idealized as an elastic bar supported by a shear foundation. As can be seen From Eqs. (1) and (6), the application of Eq. (6) to a real tire requires a knowledge of the effective stiffness ($A_s E$) of the tread region in the circumferential direction, the effective shear modulus of the side-wall region G,the effective sidewall thickness H, and the length along the mean meridional section from the rim to the intersection of the tread and carcass, A.

The extension modulus in the circumferential direction and the shear modulus of the carcass usually vary from one location to another in the meridional direction because of the orthotropic nature of the tire carcass, so some criteria must be established to compute $A_s E$ and G for a given tire section. Both the extension and shear modulus used for the results listed in this report were obtained by averaging the actual values of these properties throughout the cross-section. This technique has been successful because the variation in these properties has not been too nonlinear. However, it has a great disadvantage in a simplified analysis such as this because it requires lengthy calculations which cannot be done efficiently without the aid of a digital computer. For this reason an effort has been made to obtain some simplified, but reasonably accurate, approximations for the $A_s E$

and G necessary for calculating the fore-and-aft spring constant. The results of this effort are included in Appendix I and give a satisfactory approximate technique for calculating these properties.

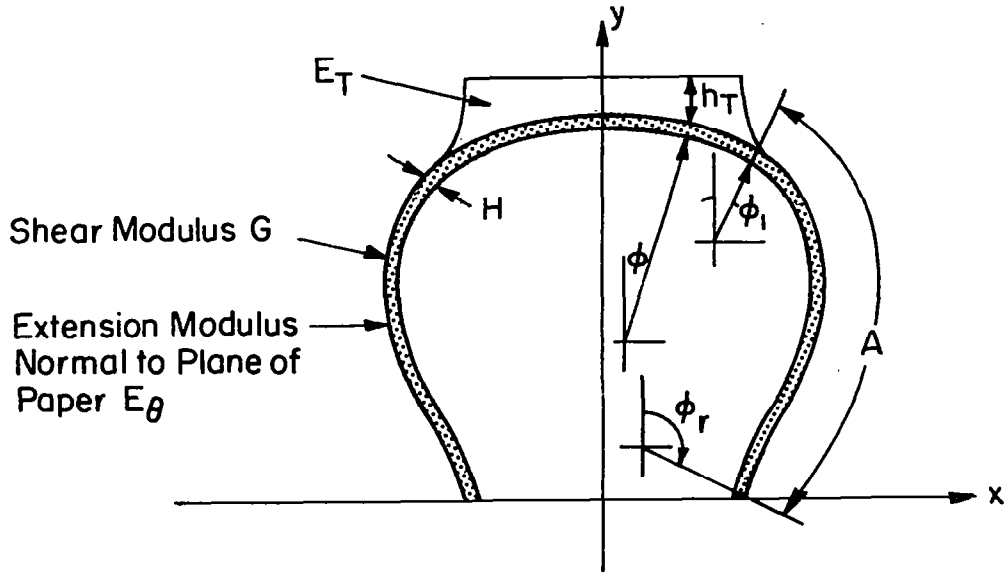

Figure 3. Meridional cross-section of the tire showing symbols used.

In order to establish some validity for the assumption that the shear foundation modulus K_s can be estimated by considering shear effects only, a simple experiment was performed by gluing a metal strip along the line of contact of two rubber cylinders placed side by side (see Figure 4). A load was attached to the bar and the resulting deflection was measured by the dial indicator. The slope of the experimental load-deflection curve, related to K_s, was then compared with the value of K_s obtained from the relation given above,

$$K_s = \frac{2GH}{A}$$

A summary of this experiment is presented below:

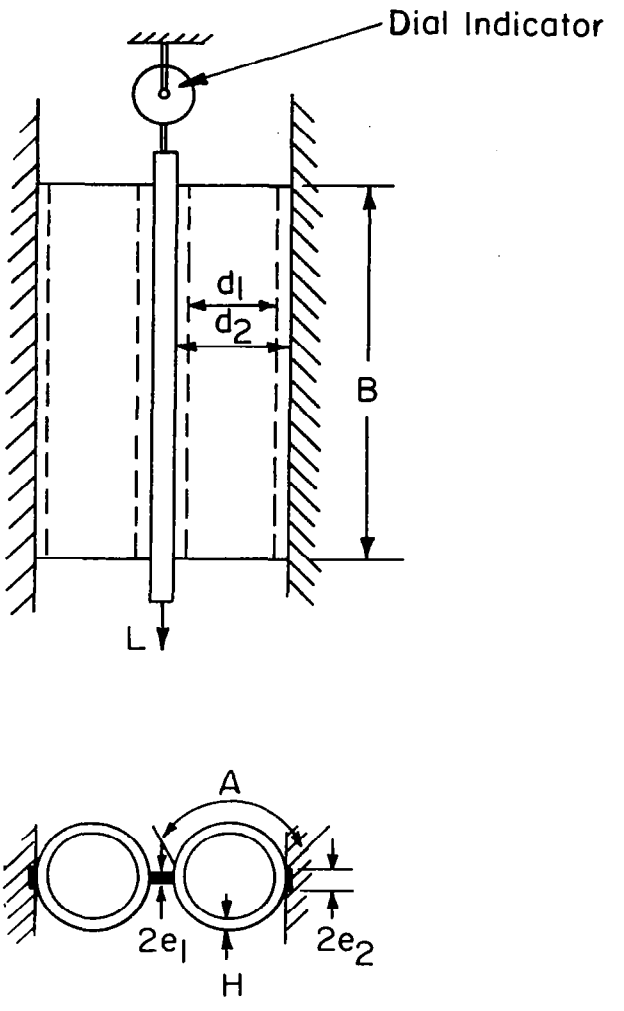

Figure 4. Experimental apparatus for checking K_s.

B	= 10.0 in.	d_2	= 1.252 in.
d_1	= 0.986 in.	H	= 0.133 in.
e_1	= 0.10 in.	A	= 1.72 in.
e_2	= 0.15 in.	G	= 200/3 lb/in.^{2}

From the test data (Figure 5), the slope of the load-deflection curve yields a K_s = 22.0 lb/in./in. The calculated value for the double tube is

$$K_s = \frac{4GH}{A} = \frac{4\left(\frac{200}{3}\right)(.133)}{1.72} = 20.6 \text{ lb/in./in.}$$

(A factor of 4 appears in this computation because of the double tube arrangement.) The close comparison between the experimental K_s and the calculated one, assuming that the foundation is flat rather than curved, indicates that any curvature effects are minor.

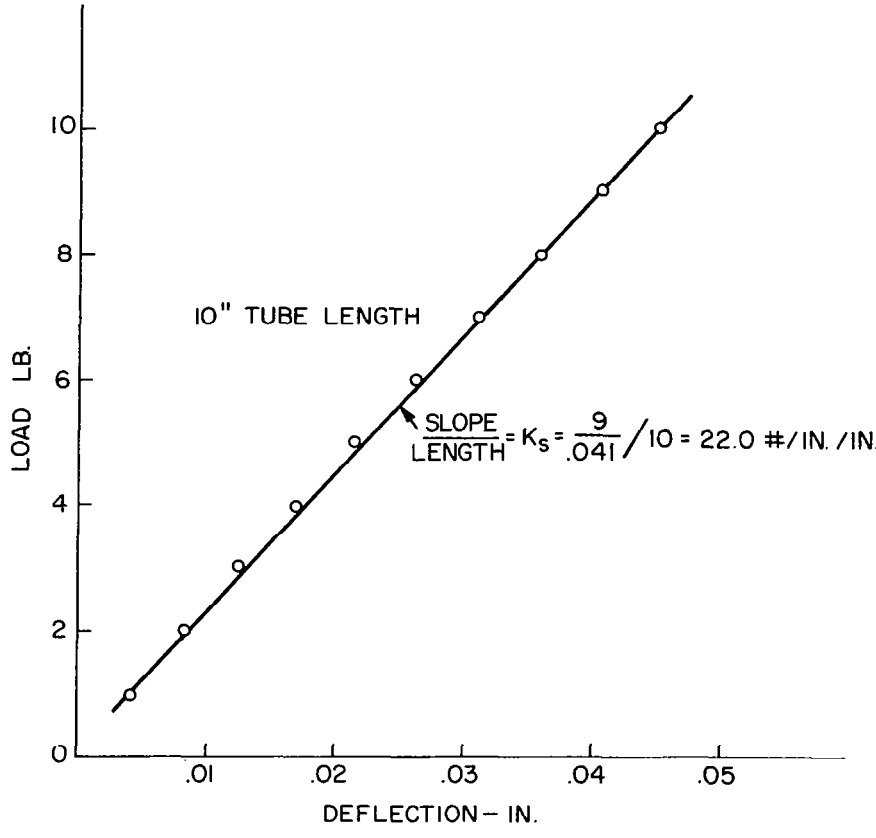

Figure 5. Load-deflection data for double tube experiment used to confirm the expression for K_s.

IV. COMPARISON OF THEORY WITH EXPERIMENT

In order to investigate the validity of Eq. (6), a series of static fore-and-aft stiffness tests were run on representative tires. Before reporting these tests and their results, the five tires used are described in detail. The idealized centerline profiles of the tires are shown in Figure 6. Tire No. 1 is a domestic 4-ply, 8.00 x 14 bias-ply tire with standard nylon cord. Tire No. 2 is a 2-ply, 7.50 x 14 bias-ply tire with standard nylon cord. Tire No. 3 is an imported 4-ply, 5.90 x 15 bias-ply tire with nylon cord. Tire No. 4 is an imported 7.50 x 14 radial-ply tire with overheads reinforced with wire cord. Tire No. 5 is a European made 155 mm x 15 in. radial-ply tire with overheads reinforced with nylon cord.

Table I is a summary of the pertinent elastic and geometric parameters required from the five tires. Using the results in this table, Figure 6, Eq. (6) and the proper elastic properties, it is possible to calculate the fore-and-aft stiffness of the five tires. Carrying out these computations gives the calculated values presented in Table II.

To check the accuracy of the calculated values, the five tires were tested in the apparatus illustrated in Figures 7 and 8. In this testing procedure the tires were loaded vertically to a fixed deflection. Then a varying fore-and-aft load was applied and the resulting deflection recorded. The slope of these load-deflection curves represents the experimental fore-and-aft spring-rates. These tests were run for different vertical deflections and inflation pressures. The results of these tests are summarized in Fig-

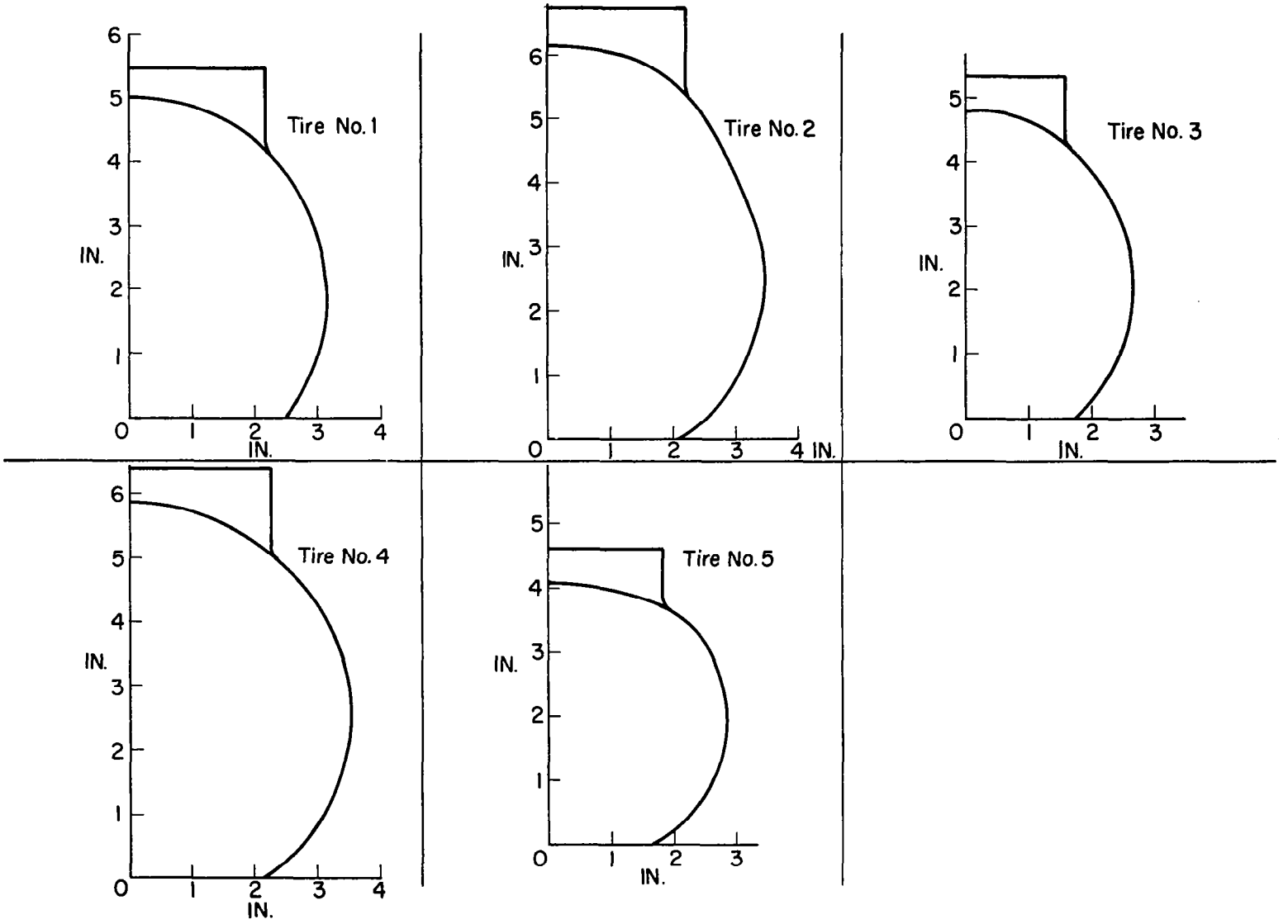

Figure 6. Idealized mid-line profiles of five pneumatic tires.

TABLE I

SUMMARY OF GEOMETRIC, ELASTIC, AND STRUCTURAL PROPERTIES OF FIVE AUTOMOTIVE TIRES

Item (Ref. 5, Table I)		Tire 1 Bias-Ply 8.00x14	Tire 2 Bias-Ply 7.50x14	Tire 3 Bias-Ply 5.90x15	Tire 4 Radial-Ply 7.50x14	Tire 5 Radial-Ply 155mm x15
AO	- outside radius of tire	12.525	13.94	12.875	13.44	12.25
L	- half circumference	39.35	43.79	40.45	42.22	38.48
ET	- extension modulus, tread rubber	670.	560.	481.	690.	490.
A	- length, mean meridional section	4.6408	5.8404	4.9217	5.7238	4.5529
H	- effective thickness for K_s	0.164	0.110	0.160	0.250	0.280
G	- effective shear modulus for K_s	28440.	47164.	43876.	269. (G_{xy})	144. (G_{xy})
A_sE	- effective spring rate, circumferential	779.	747.	760.	11906.	23027.
K_s	- spring rate, shear foundation	2010.	1747.	2852.	18.98	23.50
BETAC	- cord half angle, crown	0.6458	0.6283	0.6109	0.3142	0.2356
ROC	- radial location, crown	12.120	13.38	12.355	12.92	11.70
ROB	- radial location, rim	7.078	7.20	7.515	7.06	7.59
R	- idealized radius, sidewall	3.22	3.03	2.84	3.13	2.17
y_c	- y-coordinate, center for R	1.935	2.490	2.092	2.454	1.939
x_c	- x-coordinate, center for R	-0.057	0.465	-0.146	0.405	0.704
R1	- idealized radius, crown region	3.40	2.62	2.76	3.54	4.88
ERUB	- extension modulus, carcass rubber	438.	310.	370.	625.	300.
GRUB	- shear modulus, carcass rubber	146.	103.	123.	208.	100.
MURUB	- Poisson ratio, carcass rubber	0.500	0.500	0.500	0.500	0.500
GCORD	- shear modulus, cord	705.	705.	705.	705.	705.
AESUBC	- spring rate, cord	200.	623.	317.	350.	307.
DIAMC	- effective diameter, cord	0.025	0.040	0.026	0.025	0.023
MUC	- Poisson ratio, cord	0.700	0.700	0.700	0.700	0.700
TPLY	- effective ply thickness	0.041	0.055	0.040	0.040	0.040
NCORD	- cord count, crown	26.	19.	24.	18.	20.
ALPSTR	- normal angle, intersection	0.7746	0.6085	0.6665	0.6427	0.5775
ALPHR	- normal angle, rim	2.2148	2.5331	2.3973	2.4714	2.6792
BW	- tread width	4.36	4.40	3.20	4.60	3.68

TABLE II

SUMMARY OF EXPERIMENTAL AND CALCULATED VALUES OF K_f

Tire	K_f - lb/in.	
	Experimental	Calculated
1	2530	2503
2	2300	2286
3	2780	2944
4	1340	1469
5	1265	950

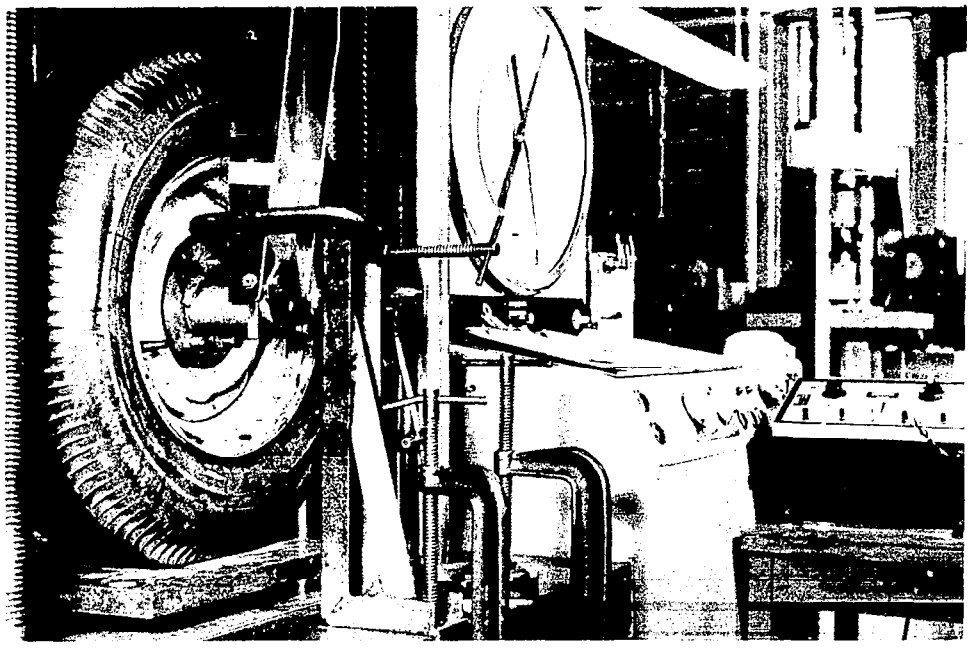

Figure 7. Photograph of experimental apparatus for K_f.

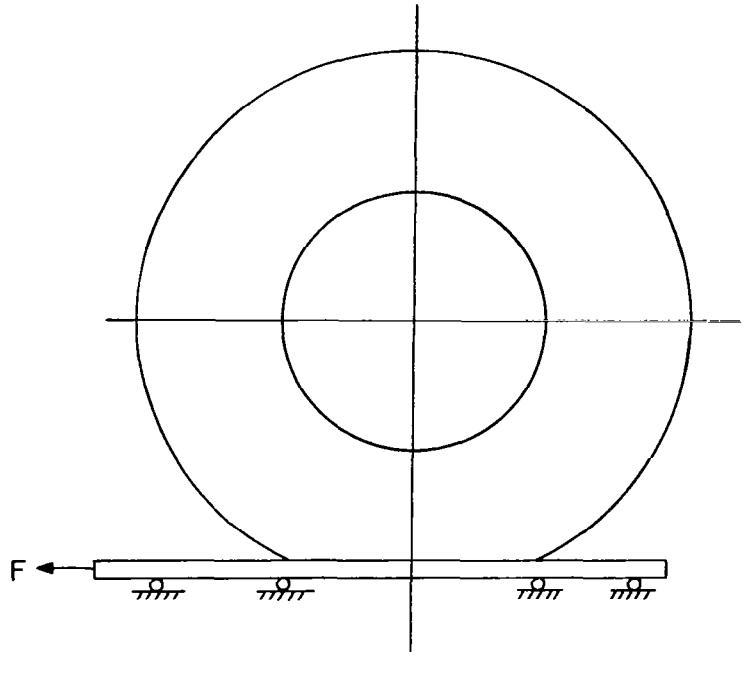

Figure 8. Schematic of fore-and-aft spring-rate test.

ures 9 through 13.

In general it can be seen from these curves that the fore-and-aft spring-rate increases only slightly with increasing vertical load and with increasing internal pressure. Since Eq. (6) does not account for the slight increase due to these factors, a comparison between the experimental and calculated results must be made in a somewhat arbitrary fashion. However, since the experimental values are nearly the same for all conditions examined, any results used as a comparison with the calculated values will serve as a meaningful check. The comparisons shown in Table II are based on experimental values obtained from vertical tire deflections of one inch and by use of manufacturers rated inflation pressure. The experimental values were determined by measuring the slopes in the linear portions of the load-deflection curves. These comparisons indicate that the simple model formulated above gives a method for approximating the fore-and-aft spring-rate of pneumatic tires using only the geometric, elastic, and structural properties required by most tire designers. At the end of the Appendix II an example problem is worked out, illustrating how an approximate fore-and-aft spring rate can be calculated if the correct input data is available.

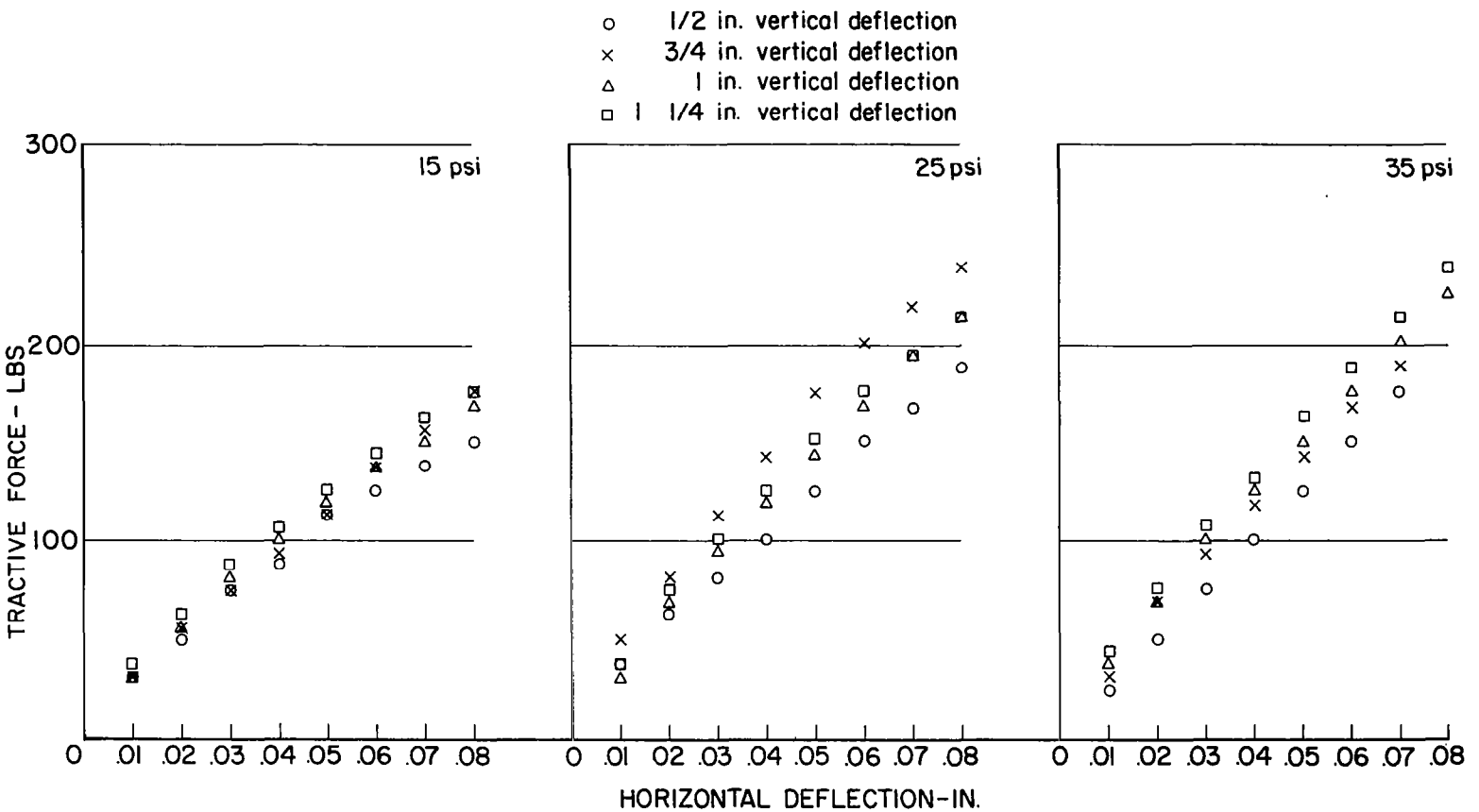

Figure 9. Fore-and-aft load-deflection curves. Tire No. 1.

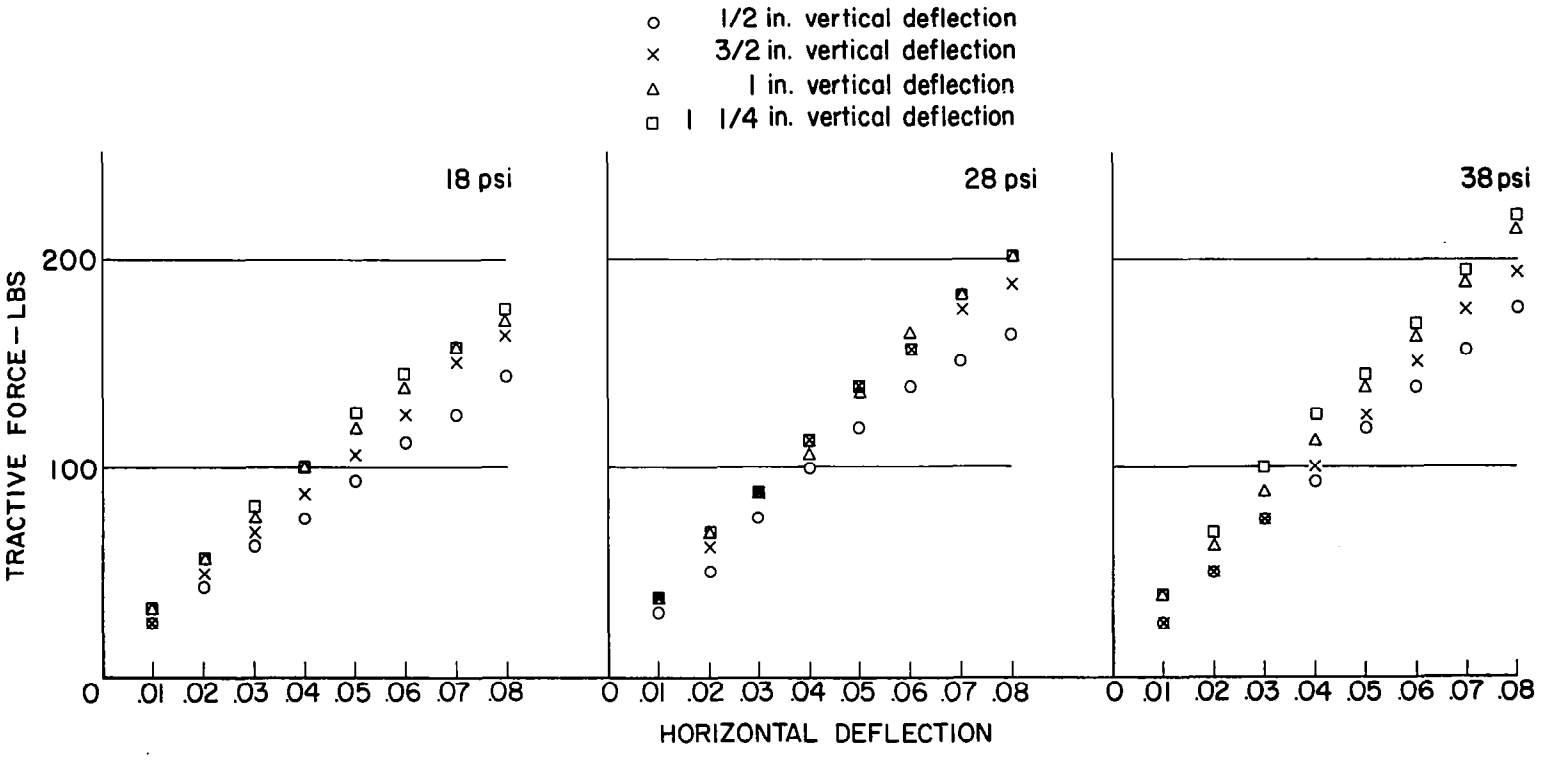

Figure 10. Fore-and-aft load-deflection curves. Tire No. 2.

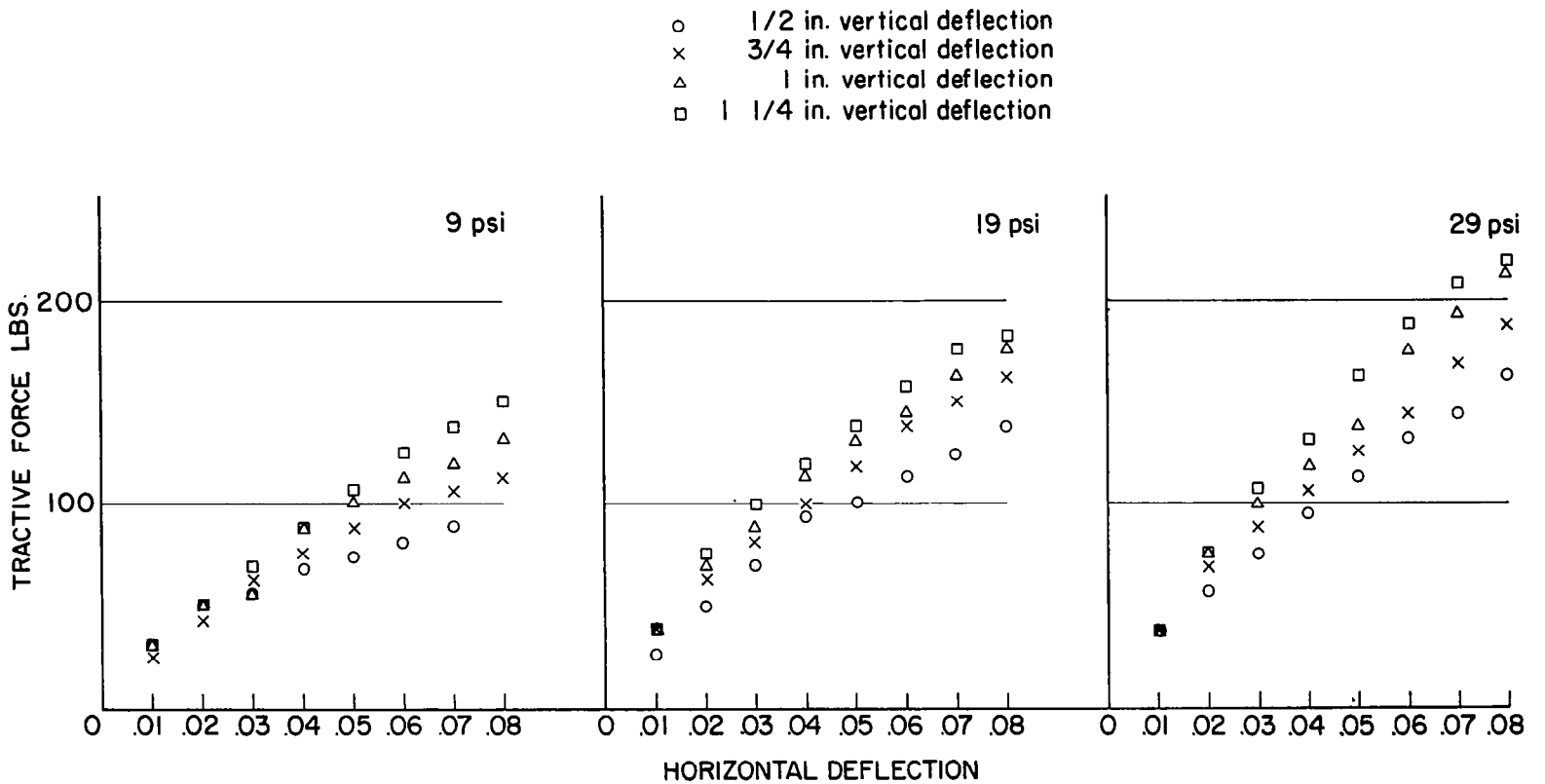

Figure 11. Fore-and-aft load-deflection curves. Tire No. 3.

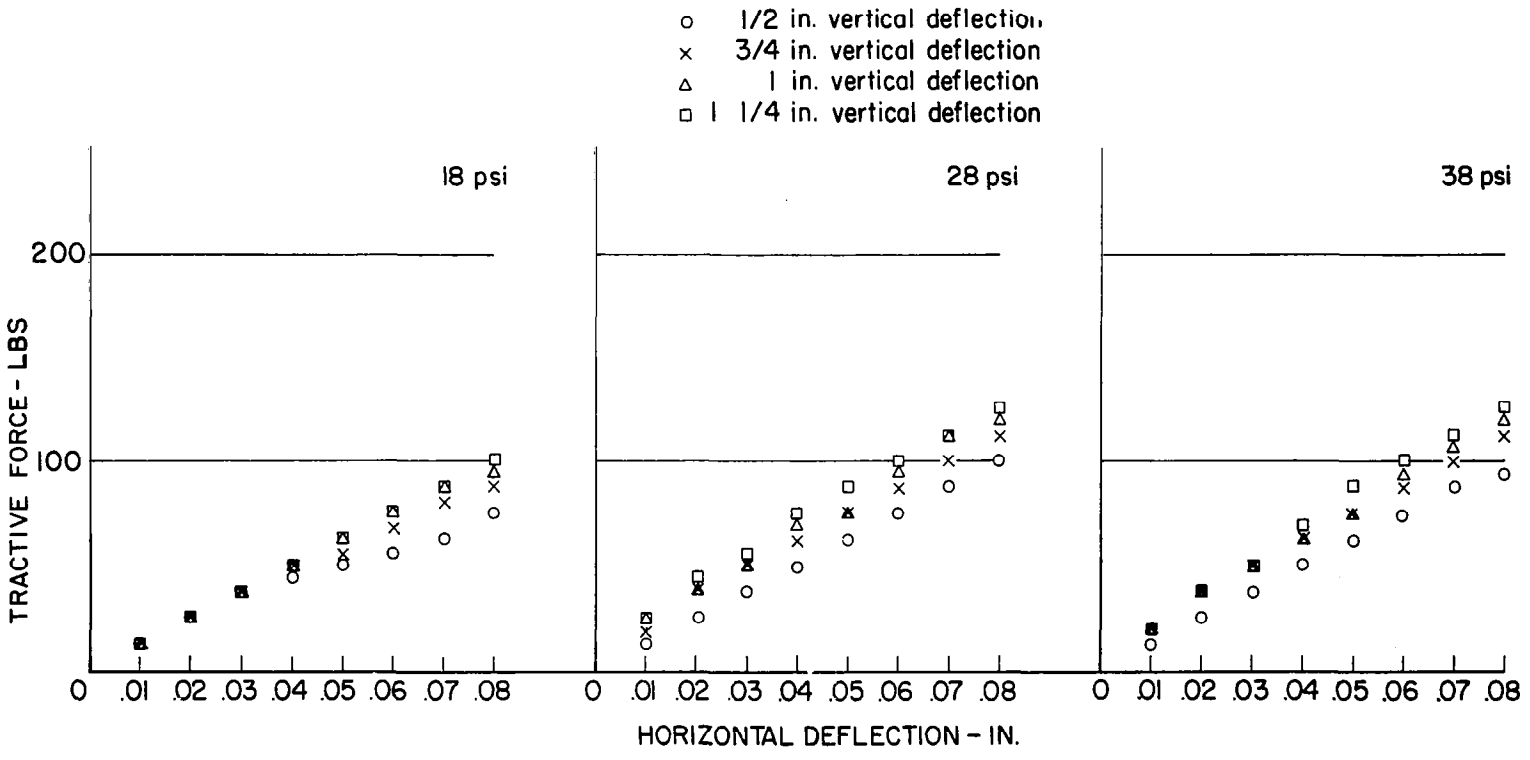

Figure 12. Fore-and-aft load-deflection curves. Tire No. 4.

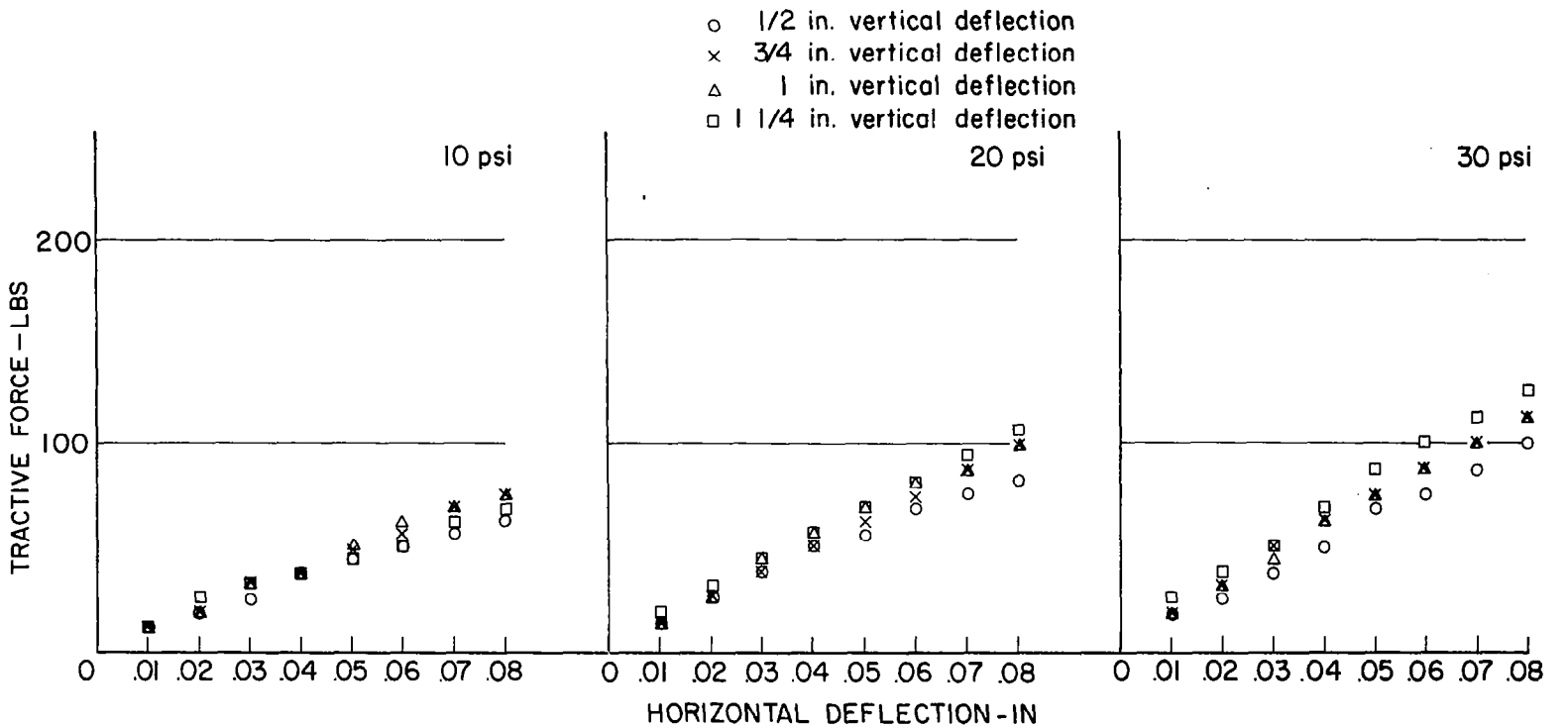

Figure 13. Fore-and-aft load-deflection curves. Tire No. 5.

V. APPENDIX I

This Appendix presents the results of an effort to simplify the computations involved in obtaining the extension modulus of the carcass in the circumferential direction, E_θ, and the shear modulus of the carcass, G.

Reference 1 gives exact expressions for the moduli of laminated orthotropic two-dimensional sheets, and these are good representations for the elastic constants of a tire carcass. However the expressions derived in Ref. 1 are quite lengthy to evaluate. They can be simplified considerably by considering the structure to be made of inextensible cords, so that the modulus of elasticity E_x, parallel to the cords in a single ply, becomes indefinitely large. By simplifying the expressions of Ref. 1 in this way, one gets

$$E_\theta = \frac{4G_{xy} \sin^2\alpha \cos^2\alpha + E_y(\cos^2\alpha - \sin^2\alpha)^2}{\sin^4\alpha} \qquad (7)$$

where α is the local cord half-angle at any meridional location, G_{xy} is the shear modulus of an individual ply and E_y is the extension modulus of an individual ply in the direction normal to the cords. This is a very good approximation for E_θ as long as the cord half-angle is not less than 30°. This is shown in Figure 14 where Eq. (7) is compared with the exact formulation of Ref. 1. Thus, Eq. (7) is a good approximation for an ordinary bias-construction tire, where the angle is almost always greater than 30°.

An approximation for the shear modulus can be obtained from a strength of materials analysis. This is reproduced in Appendix II in detail, and gives

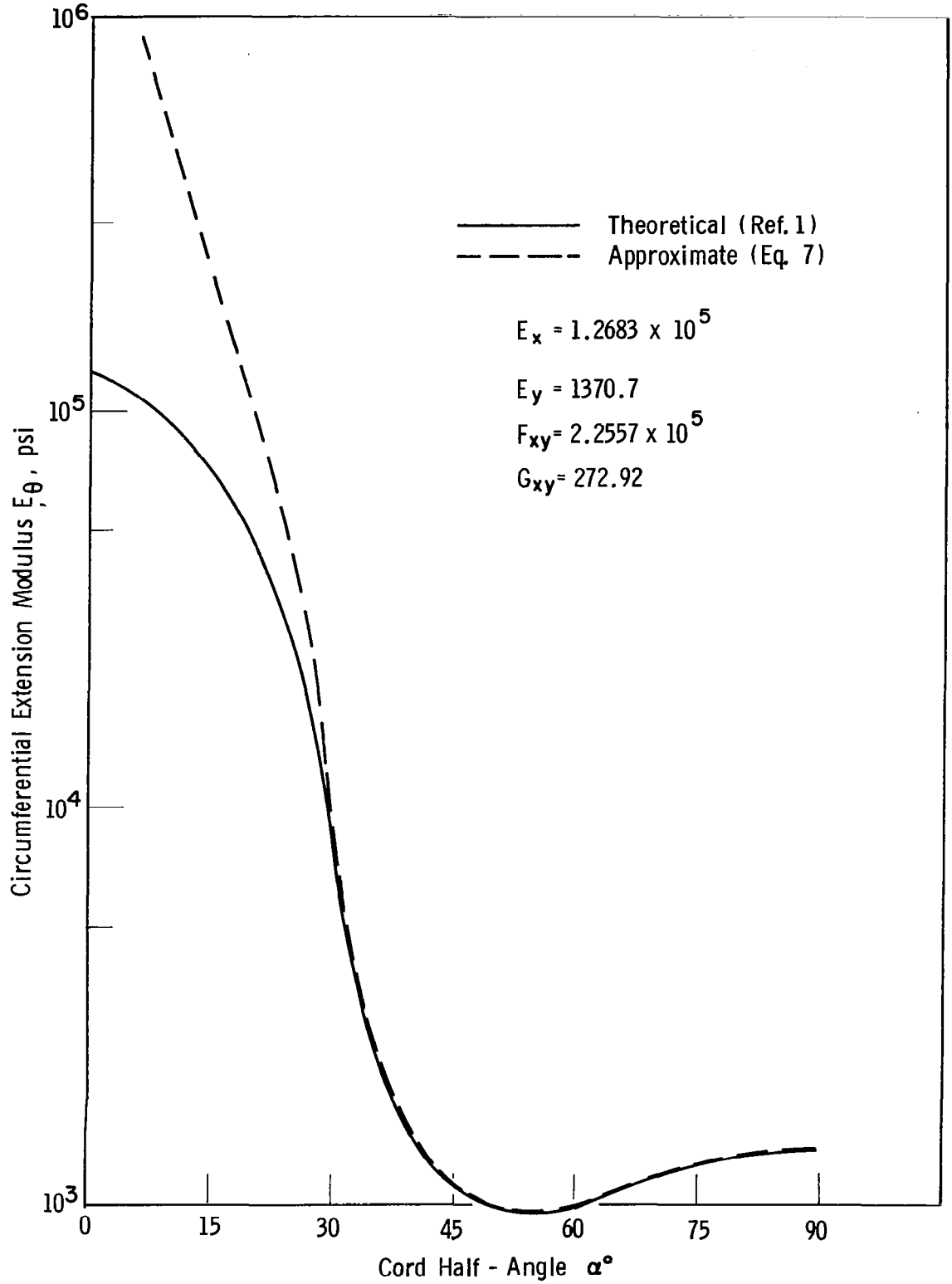

Figure 14. Comparison of exact and approximate circumferential modulus E_θ.

$$G = E_x \sin^2\alpha \cos^2\alpha \qquad (8)$$

where E_x is the extension modulus in the direction of the cords of an individual ply of the tire carcass material. This is a very good approximation for the shear modulus except at cord half-angles near 0 and 90° as shown in Figure 15 where the exact shear modulus expression from Ref. 1 is compared with Eq. (8). Again, this is valid approximation for almost all tire constructions since cord angles usually lie between 30° and 60°.

Reference 2 presents a concise method for calculating E_x, E_y, and G_{xy} as a function of the geometric and elastic properties of a single ply of the carcass material. The expressions for these moduli are listed below:

$$E_x = (AESUBC)(NCORD)/TPLY$$

$$E_y = ERUB\left[1 + 2.9\left(\frac{\lambda_H \lambda_S}{1-\lambda_S}\right)\right]$$

$$G_{xy} = 705\ K^2\lambda_H\lambda_S + GRUB(1-\lambda_S\ \lambda_H)$$

where:

$$\lambda_H = \frac{K(DIAMC)}{TPLY}$$

$$\lambda_S = K(DIAMC)(NCORD)$$

The constant k is an area coefficient equal to $\sqrt{\pi/4}$. The other parameters are defined in Table I of this report. Unfortunately both the expression for E_θ and G are still functions of the cord half-angle, α, which varies from position to position around the cross-section. However,

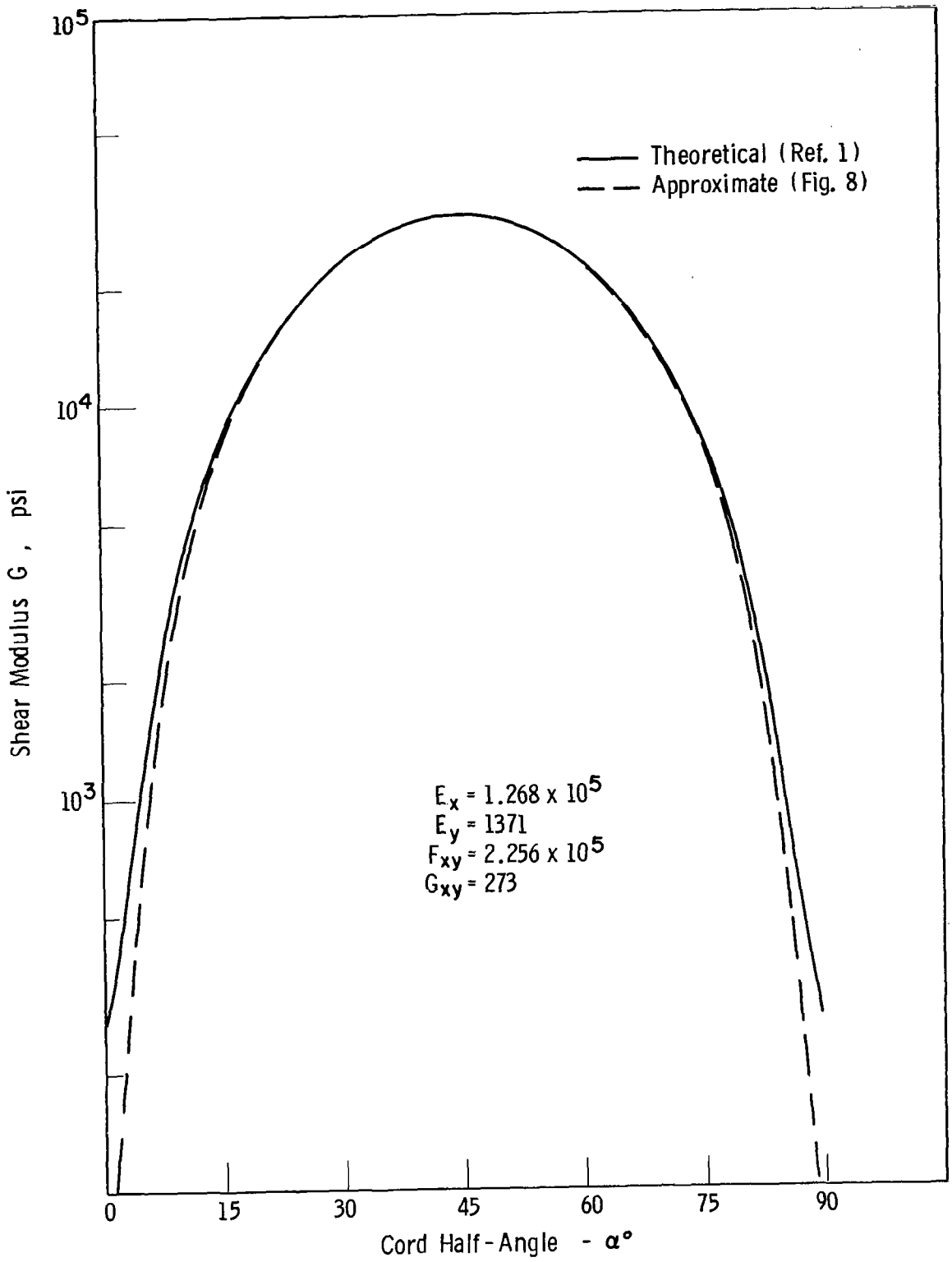

Figure 15. Comparison of exact and approximate shear modulus G.

it has been found possible to select average locations at which the values of the extension modulus and shear modulus represent useful values for the entire cross-section.

The extensional stiffness of the "bar" is represented by A_sE and primarily depends on the extensional stiffness of the carcass in the tread shoulder region of the tire. The cord half-angle in the tread and shoulder region of the tire ordinarily varies from about 35° to 45° and since the computation for E_θ is very simple at 45°, an effective E_θ is selected as the value corresponding to the value of E_θ at 45°. The total A_sE is then calculated by multiplying the E_θ at 45° by the total carcass thickness and the width of the tread. Thus,

$$A_sE = E_\theta(45°) \cdot H \cdot BW \qquad (10)$$

The shear modulus of the supporting foundation, G, is the shear modulus of the sidewall portion of the tire. Therefore G is approximated by its value at a location mid-way between the rim and the shoulder. In Figure 16 this position is noted by the dimension RS. The cord-half-angle, α_s, is approximated at this position by the "cosine law":

$$\cos\alpha_s = \frac{RS}{ROC} \cos\beta \qquad (11)$$

Where β is the cord half-angle at the crown.

The relative accuracy of these approximate moduli is examined by comparing their values with those used previously for Tires 1, 2, and 3 in Table I. These comparisons and the resulting effects on the fore-and-aft spring constant, K_f, are shown in Table III.

TABLE III

COMPARISON OF RESULTS USING APPROXIMATE MODULI

	Tire 1	Tire 2	Tire 3
G—From Table I	28440	47164	43876
G—Approx. from Eqs. (8) and (11)	29000	48500	45400
$A_s E$—From Table I	779	747	760
$A_s E$—Approx. from Eq. (7) - $\alpha = 45°$	780	580	533
K_f—From Table II	2503	2286	2944
K_f—Using Approx. A E and G	2530	2070	2520
K_f—Experimental	2530	2300	2780

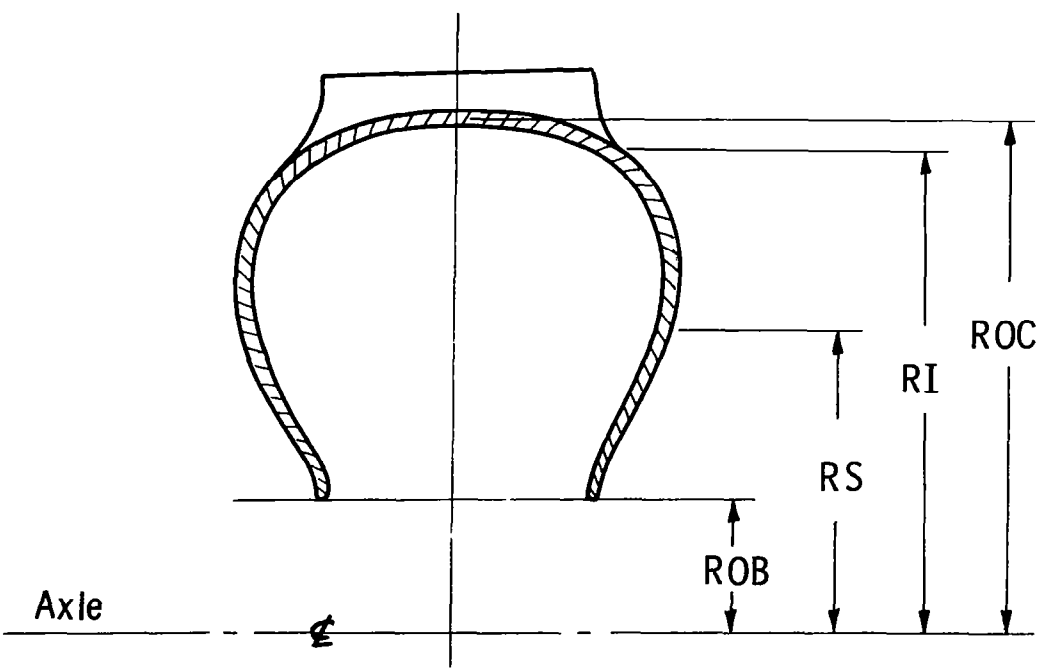

Figure 16. Sidewall location for effective G.

As can be seen, the comparisons are relatively good and since this model for calculating K_f is simple, it seems justifiable to use these simpler expressions for the moduli in approximate calculations of the spring rate K_f.

To summarize the method for calculating K_f and to illustrate the relative ease with which it can be done if one uses the approximate moduli outlined above, an example problem is given below.

PROBLEM STATEMENT

Calculate an approximate fore-and-aft spring rate for the tire described in Figure 17. This tire roughly corresponds to a standard 9.50 by 14 four-ply tire.

The elastic properties of the individual ply are calculated first by referring to Eqs. (9):

$$\lambda_H = \frac{\sqrt{\frac{\pi}{4}}(.028)}{(.033)} = 0.758$$

$$\lambda_s = \sqrt{\frac{\pi}{4}}(.028)(20) = 0.500$$

$$E_x = (300)(20)/(.033) = 1.82 \times 10^5 \text{ psi}$$

$$E_y = 550\left[1 + 2.9\left(\frac{0.758 \times 0.500}{1 - 0.500}\right)\right] = 1760 \text{ psi}$$

$$G_{xy} = 705(0.7854)(0.758)(0.500) + 180\,(1-0.758 \times 0.500)$$

$$= 325 \text{ psi}$$

The extension modulus E_θ is then computed from Eq. (7), using $\alpha = 45°$:

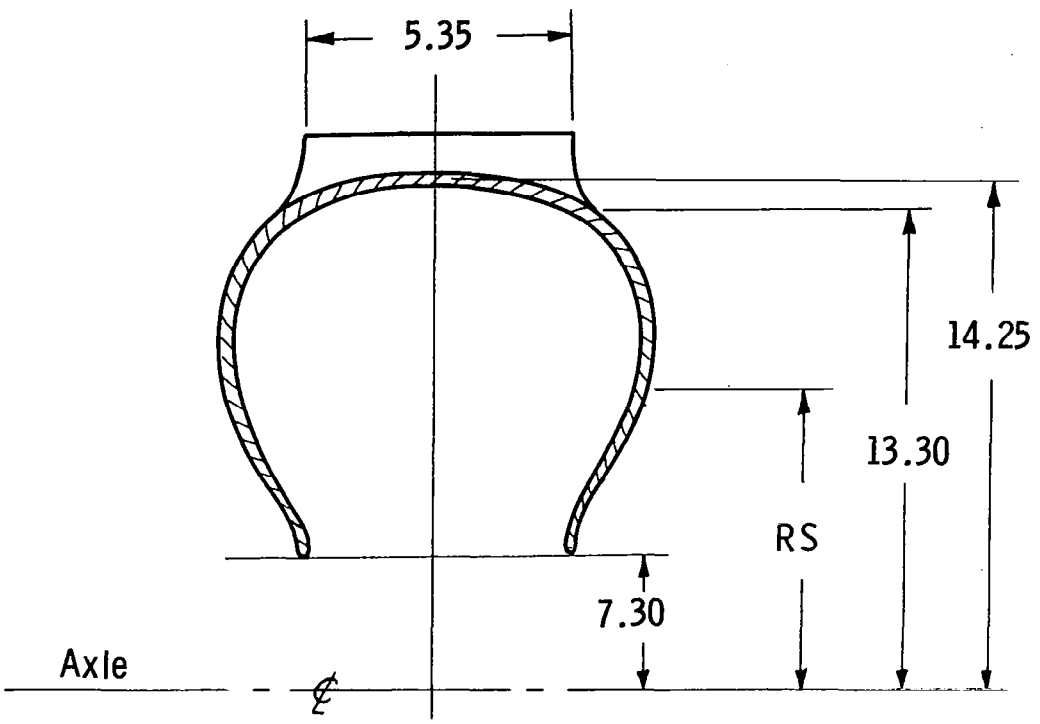

AESUBC = 300 lb/ in.	NCORD = 20 ends/in.	TPLY = 0.033 in.
ERUB = 550 psi	GRUB = 180 psi	H = 0.132 in.
BW = 5.35 in.	β = 37.5°	ROB = 7.30 in.
ROC = 14.25 in.	RI = 13.30 in.	A = 9.70 in.
DIAMC = 0.028 in.	a = 14.83 in.	

Figure 17. Description of hypothetical tire for example problem.

$$E_\theta = 4(325) = 1300 \text{ psi}$$

Thus $A_s E$ can be found from Eq. (10):

$$A_s E = 1300(0.132)(5.35) = 915 \text{ lb}$$

The next property to calculate is G, whose mean value is found at a location approximately half way between the rim and the shoulder. The radial location RS is determined by locating the point half way between ROB and RI (see Figure 16), which for this example is:

$$RS = \frac{RI + ROB}{2} = \frac{7.30 + 13.30}{2} = 10.30 \text{ in.}$$

The cord half-angle at this location is found from Eq. (11):

$$\cos \alpha_s = \frac{10.30}{14.25} \cos 37.5° = 0.573$$

and $\sin \alpha_s = 0.819$. Thus from Eq. (8):

$$G = 1.82 \times 10^5 (0.573)^2 (0.819)^2 = 4.00 \times 10^4 \text{ psi}$$

Now referring to Eq. (6), the fore-and-aft spring rate is

$$K_f = 2(A_s E)(q)(\tanh qa)$$

The value for q is found from Eq. (1) and the definition of K_s:

$$K_s = \frac{2GH}{A} = \frac{2(4.00 \times 10^4)(0.132)}{9.90} = 1070 \text{ lb/in./in.}$$

$$q = \sqrt{\frac{1070}{915}} = 1.08/\text{in.}$$

Therefore, the spring rate is

$$K_f = 2(915)(1.08)(1) = 1980 \text{ lb/in.}$$

VI. APPENDIX II

Consider a plane element made up of a series of parallel cords, with end count n, each carrying a tension load T_o as shown below.

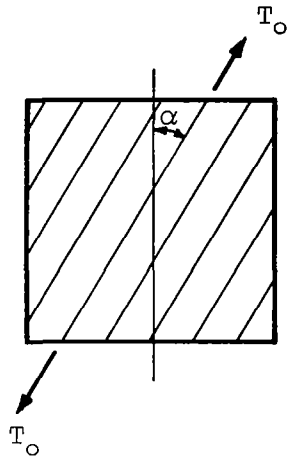

The number of cords per unit length on the upper and lower faces is $n \cdot \cos \alpha$. The tension component per cord tangential to the upper or lower faces is $T_o \sin \alpha$. Hence, the shear force per unit length is

$$T_o \sin \alpha \cdot n \cos \alpha.$$

If the thickness of the lamina is h, then the shear stress τ, which by equilibrium acts on all edges equally, is

$$\tau = T_o \frac{n}{h} \sin \alpha \cos \alpha \qquad (12)$$

Now consider deformation of the element shown above in the shear direction, based on the concept that the cord will elongate under tension T_o.

From the geometry,

$$x \sin \alpha = \epsilon \ell_o$$

where ϵ is cord strain, ℓ_o the original cord length.

$$x = \epsilon \ell_o / \sin \alpha .$$

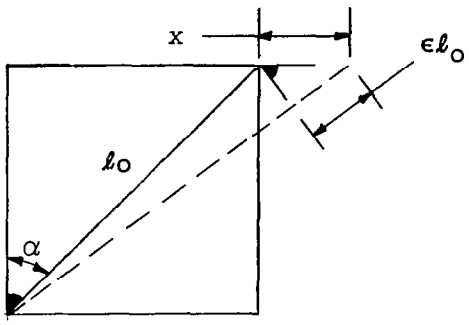

But shear strain is defined as

$$\gamma = \frac{x}{\ell_o \cos \alpha} = \frac{\epsilon \ell_o}{\ell_o \sin \alpha \cos \alpha} = \frac{\epsilon}{\sin \alpha \cos \alpha} \quad (13)$$

Also, cord tension and strain are related by the cord spring rate

$$T_o = (AE)_c \cdot \epsilon$$

Hence, shear modulus G is

$$G = \frac{\tau}{\gamma} = \frac{T_o \frac{n}{h} \sin \alpha \cos \alpha}{T_o} / (AE)_c \sin \alpha \cos \alpha$$

$$= (AE)_c \frac{n}{h} \sin^2 \alpha \cos^2 \alpha \quad (14)$$

But the extension modulus parallel to the cords is $(AE)_c \frac{n}{h} = E_x$, so that

$$G = E_x \sin^2 \alpha \cos^2 \alpha \quad (15)$$

VII. ACKNOWLEDGMENTS

The authors wish to thank Mr. B. Bourland, Mr. P. A. Schultz, and Mr. B. Bowman for their assistance in obtaining the experimental data presented in this report.

VIII. REFERENCES

1. Clark, S. K., "Internal Characteristics of Orthctropic Laminates," Textile Research Journal, Vol. 33, No. 11, Nov. 1963.

2. Clark, S. K., Dodge, R. N., Field, N. L., "Calculation of Elastic Constants of a Single Sheet of Rubber-Coated Fabric," The Univ. of Michigan, ORA Technical Report 02957-14-T, Feb. 1962.

3. Smiley, R. F., and Horne, W. B., "Mechanical Properties of Pneumatic Tires with Special Reference to Modern Aircraft Tires," NACA Technical Note 4110, National Advisory Committee for Aeronautics, Washington, D.C., January, 1958.

4. Clark, S. K., "Simple Approximations for Force-Deflection Characteristics of Aircraft Tires," NASA Contractor Report, NASA CR-439, Washington, D.C., May, 1966.

5. Dodge, R. N., "Prediction of Pneumatic Tire Characteristics from a Cylindrical Shell Model." Paper presented at SAE Mid-Year Meeting, Chicago, May 1965.

6. Clark, S. K., "An Analog for the Static Loading of a Pneumatic Tire." Paper presented at SAE Mid-Year Meeting, Chicago, May 1965.

7. Tielking, J. T., "Plane Vibration Characteristics of a Pneumatic Tire Model." Paper presented at SAE Mid-Year Meeting, Chicago, May 1965.

NASA-Langley, 1967 —— 32 CR-900